21 June 1996

ELSEVIER

Chemical Physics Letters 256 (1996) 43–50

CHEMICAL PHYSICS LETTERS

# $Ar_2^+$ molecules in intense laser fields

Christof Wunderlich [1], Hartmut Figger, Theodor W. Hänsch

*Max-Planck-Institut für Quantenoptik, D-85748 Garching, Germany*

Received 29 January 1996; in final form 1 April 1996

**Abstract**

We have studied the interaction between intense laser fields ($\leqslant 7 \times 10^{12}$ W/cm$^2$) and molecules. For the diatomic molecular ion $Ar_2^+$ the number of photofragments as a function of laser intensity can be quantitatively explained in terms of light-induced adiabatic molecular potentials. The effects predicted by this model tend to cancel under realistic experimental conditions with a thermal distribution of the rovibrational populations. This molecular beam experiment allows for a fully quantitative comparison with theory, since only one dissociation channel is operative and all parameters relevant for a computational simulation have been determined.

## 1. Introduction

Using laser light not only as a spectroscopic tool, but to manipulate atoms and molecules on a microscopic scale has opened up a fascinating field of research in recent years. Additional internal degrees of freedom of molecules, as compared to atoms, lead to intriguing dynamical behavior in a coherent light field. With the help of intense, short-pulse lasers it has become possible to induce electronic Rabi frequencies in molecules comparable to the frequency of the vibrational motion of the nuclei and thus to decidedly influence intramolecular dynamics. New phenomena arising in intense laser fields have been predicted in numerous theoretical studies (e.g. Refs. [1–15]).

On the experimental side it has proven to be difficult to identify these new effects. Most experimental investigations of molecules in intense laser fields have used neutral molecules as a starting point, and both ionization and dissociation of the molecule and of its ions occurred during one laser pulse [2,28–25]. The presence of several possible ionization and dissociation channels complicates the interpretation of these studies [2]. In a recent experiment the transient absorption of TlJ was interpreted in terms of an avoided crossing between molecular dressed states [26].

In this Letter we report the results of an experiment employing a mass selected molecular beam of $Ar_2^+$ that allows a fully quantitative comparison with theoretical predictions concerning molecules in intense laser fields. We chose photofragment spectroscopy to diagnose how an intense field affects the intramolecular dynamics of this model molecule. All the parameters necessary for a quantitative simulation of the experiment have been determined, including the relevant potential curves of $Ar_2^+$ and the dipole moment coupling them. No ambiguity arises as to the origin of the detected photofragments, since only one dissociation channel is operative. Competing processes, most importantly ionization and multiphoton dissociation, are ruled out experimentally. Under these experimen-

[1] Present address: Laboratoire Kastler Brossel, Departement de Physique de l'Ecole Normale Superieure, 24 rue Lhomond, F-75231 Paris Cedex 05, France.


*PII* S0009-2614(96)00418-6

tal conditions the unambiguous identification of new strong field effects can be expected. Indeed, the results presented here can be quantitatively explained using light-induced molecular potentials (LIP). Using this theoretical approach to model the behavior of a molecule in a light field allows for an intuitive explanation of new phenomena arising in strong fields (see Section 2).

The model of LIP predicts drastic strong field effects for each individual vibrational level. Under realistic experimental conditions with a thermal distribution of the population of rovibrational levels the characteristic behavior of a single level is not observable, but one should still be able to observe an integral effect predicted by LIP for the net absorption of one photon. Surprisingly, it turns out that for the strong field results presented in this Letter the "classical" approach, i.e. Fermi's golden Rule (FGR) for one-photon-processes, is equally well suited to describe the experiment. Since *all* experimental parameters have been determined, it is possible to resolve the paradox why Fermi's golden rule gives correct results when driving a strong optical dipole transition in a molecule with such high intensities ($\leqslant 8 \times 10^{12}$ W/cm$^2$).

In Section 2 the model of light-induced molecular potentials will be outlined and characteristic new phenomena predicted by this theory for $Ar_2^+$ in a strong laser field are introduced. Then, after a short account of the experimental apparatus in Section 3, the measured number of photofragments as a function of laser intensity will be interpreted in Section 4 with the help of these two (LIP and FGR) theoretical approaches.

## 2. Light-induced molecular potentials

If one uses light-induced molecular potential curves (field-electronic states [1]) to describe intramolecular dynamics in laser fields, strong field effects can be intuitively interpreted. Here, we will consider the model case of the diatomic molecule $Ar_2^+$ with two electronic states that are characterized by a bonding and an anti-bonding potential curve. Exposing this molecule to laser light of frequency $\omega_L$ shifts the energy of the lower, bonding potential curve by $\hbar\omega_L$, if the interaction between molecule and electromagnetic field is described in a dressed state representation. Thus the two diabatic potential curves shown as

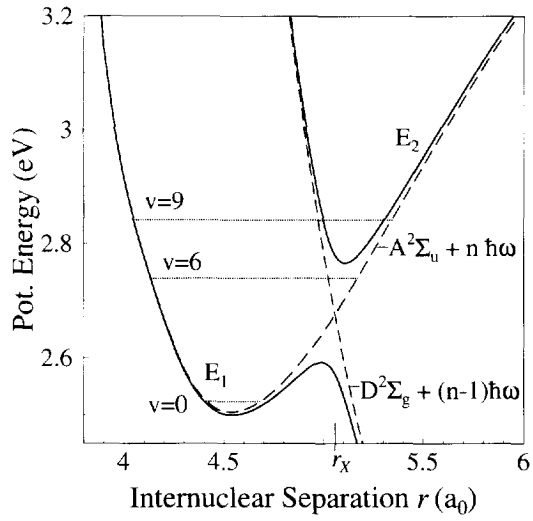


Fig. 1. Light-induced adiabatic potential curves (solid lines) in $Ar_2^+$ at a laser wavelength of 495 nm and intensity of $10^{12}$ W/cm$^2$. Dashed lines symbolize diabatic potential curves, due to the ground state $A^2\Sigma_u^+$ shifted by $\hbar\omega$ and the anti-bonding $D^2\Sigma_g^+$ state. Dotted lines indicate the positions of two diabatic vibrational levels.

dashed lines in Fig. 1 cross at the internuclear distance, $r_X$, where the two electronic states are coupled resonantly by the light field. Taking into account the dipole interaction (proportional to $\sqrt{I}$, $I$ being the laser intensity) induced by the light field, brings about a repulsion between the diabatic curves and one obtains adiabatic light-induced potentials, $E_1$ and $E_2$, illustrated by solid lines in Fig. 1. The characteristic features of these new electronic states can be changed by varying the frequency and intensity of the laser field. Increasing the frequency, for example, moves the avoided crossing to a smaller internuclear distance $r_X$. The "gap" between the adiabatic curves can be given a desired size by adjusting the intensity of the light field.

Three observable phenomena due to the presence of new light-induced potentials, $E_1$ and $E_2$, are expected if one chooses photofragment spectroscopy as a diagnostic tool. They depend on the initial rovibrational energy of the nuclei characterized by vibrational quantum number $v$ and rotational quantum number $K$: (i) Tunneling through the potential barrier of the lower of the adiabatic potentials, $E_1$ (e.g. $v = 0$). Furthermore, the binding energy of vibrational levels below the lo-

cal maximum of $E_1$ is considerably lowered compared to the "natural" molecule. (ii) Some levels with vibrational energy above the avoided crossing exhibit an increased dissociation probability due to the presence of the gap between $E_1$ and $E_2$ (e.g. $v = 9$). (iii) Other levels become trapped in the upper of the light-induced electronic states, $E_2$, and thus stabilize in an intense field. These phenomena are due to the net absorption of one photon. Each of them changes the dissociation probability as a function of intensity for a given vibrational level in a characteristic way. This, in turn, can be diagnosed by measuring the number of photofragments and their energy and angular distribution.

Fig. 2 illustrates the effects of light-induced potentials on the dissociation rate for three vibrational levels ($v = 0, 6, 9$). Solid lines show the dissociation rate, $R_{\omega,v,K}(I)$, that is predicted, if one uses light-induced adiabatic potentials in the rotating wave approximation (one-photon coupling, Fig. 1). The diabatic electronic states one starts with when calculating $R$ are the ground state $A\,^2\Sigma_u^+$ and the excited state $D\,^2\Sigma_g^+$ of $Ar_2^+$ (Fig. 1). In the dressed state representation the lower potential curve $A\,^2\Sigma_u^+$ is shifted up by the energy of one photon. The two crossing diabatic curves are coupled via the electric dipole interaction with the light field. After diagonalizing the $2 \times 2$ matrix with the electronic eigenvalues as a function of the internuclear distance on the diagonal places and the dipole interaction on the off-diagonal places one obtains adiabatic potential curves $E_1$ and $E_2$ (solid lines in Fig. 1) [1]. The rate of dissociation can now be determined, for example, by applying the well-known Landau–Zener formula [29] to this curve crossing problem. However, the use of this formula gives good results only for vibrational energies above the avoided crossing. Zhu and Nakamura have derived modified expressions of the Landau–Zener formula that are valid over a wide range of coupling strengths and for all vibrational energies [30]. Calculating the transmission probability $p$ of a particle through the adiabatic potential system and dividing $p$ by the vibrational period, $\tau$, yields the rate of dissociation, $R$. It depends on the shape of $E_1$ and $E_2$ and thus on the frequency of the laser. Dashed lines in Fig. 2 give for comparison the dissociation rate obtained from Fermi's golden rule for one-photon absorption ($A\,^2\Sigma_u^+ \xrightarrow{\hbar\omega_L} D\,^2\Sigma_g^+$).

These two approaches yield the same result at low

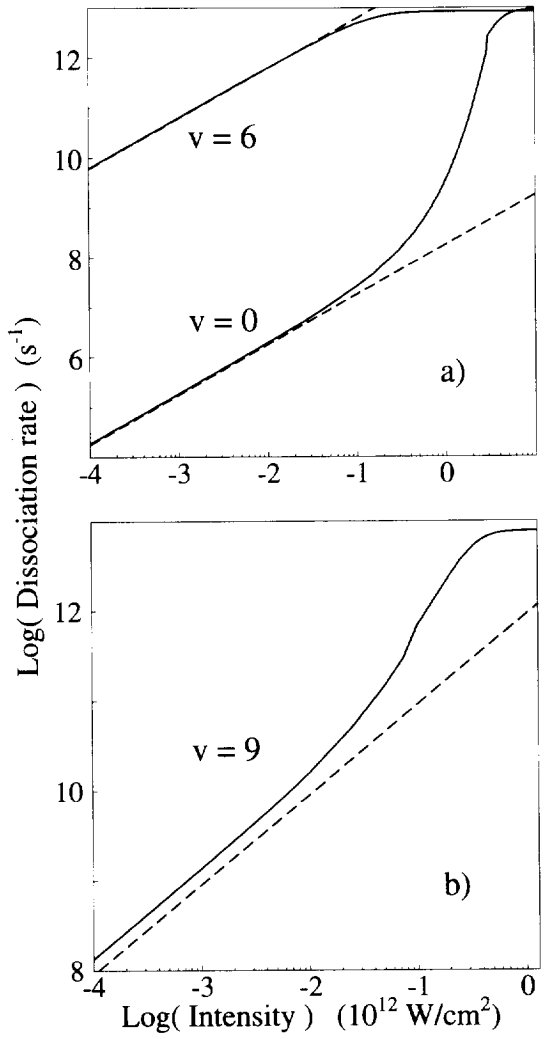


Fig. 2. Dissociation rate of $Ar_2^+$ as a function of laser intensity. Dashed lines represent calculations using Fermi's golden rule, whereas solid lines stand for a calculation using light-induced adiabatic potentials (both for one-photon absorption). (a) $v = 0, 6$. (b) $v = 9$. $v$ denotes the vibrational quantum number.

laser intensities. For vibrational quantum number $v = 0$ and $I \gtrsim 10^{11}\,\mathrm{W/cm^2}$, however, the solid line deviates strongly from the golden rule result due to an increasing probability for tunneling through the diminishing potential barrier of $E_1$ (case i). At an intensity of $10^{13}\,\mathrm{W/cm^2}$, the potential barrier is completely suppressed and the probability, $p$, for dissociation of the $v = 0$ level equals 1 (Fig. 2a). The $v = 9$ level is strongly affected by the gap opening up between $E_1$

and $E_2$ as the laser intensity increases beyond $\approx 10^{10}$ W/cm$^2$ (case (ii), Fig. 2b).

Vibrational states in the immediate vicinity of the crossing between diabatic potential curves exhibit a high dissociation probability and become completely unbound when, with increasing intensity, their energy falls in the potential gap between the local maximum of $E_1$ and the minimum of $E_2$ (e.g. $v = 6$ in Fig. 1). In particular, the local maximum (barrier) of $E_1$ diminishes with increasing intensity and vibrational levels *below* the diabatic crossing that lie at low intensity below the top of this barrier find themselves in the gap region at a higher laser intensity. At an intensity of $10^{12}$ W/cm$^2$ (Fig. 1), for example, levels with vibrational quantum number $v \geqslant 3$ can escape over this barrier and dissociate quickly. This has been termed "bond-softening" [18]. While the barrier of $E_1$ drops lower and lower with increasing intensity, the minimum of $E_2$ is pushed upwards more and more. Levels *above* the diabatic crossing also find themselves in the potential gap between $E_1$ and $E_2$ and are also characterized by high dissociation rates. Treating the levels in the gap region with Fermi's golden rule yields a similarly high dissociation rate as the LIP model. This is due to the large Franck–Condon overlap with the excited state. In fact, both models predict indistinguishable behavior for vibrational states in the vicinity of the avoided crossing under the conditions (laser pulse length and intensity) of this experiment.

The third phenomenon (trapping in $E_2$) is expected to be observable if the molecules experience laser pulses with a short risetime. In the interpretation of our data this does not play a role, because of the relatively slow risetime of the pulses ($I(t) = I_0 \exp(-2t^2/t_0^2)$, $t_0 \gtrsim 15$ ps). If the laser intensity rises slowly, then the gap between the adiabatic curves opens up slowly. Molecules that were at the beginning of the pulse confined to $E_2$, are still likely to be dissociated since, each time the nuclei pass the avoided crossing while the intensity still rises, there is a non-zero probability to "jump" over this gap.

## 3. Experimental

$(^{40}Ar^{40}Ar)^+$ molecules are generated in a dc-discharge (duoplasmatron), accelerated to an energy of 7.5 keV, and then separated from other ions contained initially in the beam with a sector magnet [28]. The density distribution of $Ar_2^+$ molecules in the beam (typically 20 nA ion current, radius of 0.7 mm) is measured immediately before the interaction region. After the mass selected molecular beam has been collimated, it crosses at right angles a focused dye laser beam. Even though the laser pulse length is $\approx$30 ns, the molecules experience pulses in the picosecond region ($\gtrsim$ 30 ps) determined by the time needed to traverse the focal region. A lens doublet (f-number 4.3) focuses the Gaussian laser beam to a diffraction limited waist size. Imaging of the focal region of the laser beam onto a CCD camera confirmed the calculated beam parameters. Charged photofragments ($Ar^+$ ions) and $Ar_2^+$ molecules are removed from the molecular beam after the interaction zone by means of electrostatic deflection plates, and $Ar^+$ ions are counted using a secondary electron multiplier whose detection efficiency is known. A position sensitive, optically read out, multichannel plate detector is used to detect neutral photofragments (Ar atoms) which yields a 2-dimensional projection of the 3-d momentum distribution of the photofragments in their center-of-mass frame. A more detailed description of this detection scheme will be given in a subsequent publication.

## 4. Discussion of experimental results

Fig. 3a shows the number of $Ar^+$ photofragments as a function of laser intensity at a laser wavelength of 495 nm. Each data point stands for the average signal of 8000 to 21000 laser pulses. The lower abscissa gives the peak intensity experienced by the molecules whereas the peak energy/area per laser pulse is indicated on the upper abscissa. Solid lines in Fig. 3 show the result of a computational simulation of the experiment. In this simulation (discussed later), light-induced molecular potentials are used as a starting point. The parameters employed in the computation were, without exception, established experimentally. Thus, a meaningful quantitative comparison between theoretical predictions of the behavior of molecules in intense laser fields and experimental results is possible. The data depicted in Fig. 3b were taken under the same conditions as the data in Fig. 3a except at a longer laser wavelength (535 nm) so that the avoided

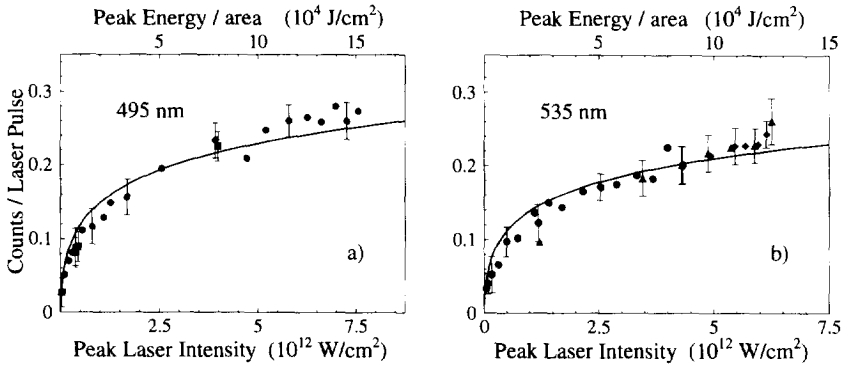


Fig. 3. Number of dissociated $Ar_2^+$ molecules as a function of laser intensity at two wavelengths. Each data point stands for the average number of counts of 8000 to 21000 laser pulses. The solid line symbolizes the result of a computational simulation using light-induced potential curves. All parameters of the simulation were determined experimentally.

crossing (Fig. 1) shifts towards a larger internuclear separation. Again, there is fair agreement between the theory of light-induced molecular states and the experiment.

The model of light-induced potentials as compared to Fermi's golden rule predicts dramatic changes in the dissociation probability with intensity for individual vibrational levels (compare Fig. 2).

In Refs. [18,19] the term "bond-softening" has been coined and was used to describe the enhanced dissociation of molecules with a kinetic energy of the nuclei that corresponds to a diabatic vibrational level above the barrier of $E_1$ (Fig. 1) and *below* the diabatic crossing. Levels *above* this crossing also dissociate very quickly. (compare Section 2 and Fig. 2, $v = 6$). Vibrational levels in the energy range between the two light-induced adiabatic potentials $E_1$ and $E_2$ ($v = 3...8$ in Fig. 1), in the vicinity of the avoided crossing, are characterized by high dissociation rates already at moderate intensities, as predicted by both the model of light-induced potentials and Fermi's golden rule (see Fig. 2a, $v = 6$).

Calculations (assuming realistic experimental conditions) do not give distinctive results for these levels when employing the two theoretical models with laser pulses lasting between a few tens and a hundred picoseconds as they were used here and for the experiments reported in Refs. [18,19]. Since these levels are appreciably populated in our experiment at $kT = 0.10$ eV, they dominate the photodissociation signal and tend to obscure the dramatic effects expected from vibrational states below and above the avoided crossing. Indeed, a simulation with $R$ calculated from Fermi's golden rule agrees equally well with the experimental data as do the solid curves shown in Fig. 3. "Bond-softening", therefore, does not lead to new effects in photodissociation due to the net absorption of one photon in an intense laser field. Also, vibrational levels not too far *above* the diabatic crossing exhibit a similar behavior and are characterized by dissociation rates that do not allow a distinction between the models in question with the laser parameters (intensity and pulse length) employed here and in Ref. [18].

The appearance of photofragments with low kinetic energy at high laser intensities (e.g. Ref. 14) is not a phenomenon that is particular to "bond-softening". Vibrational levels in the immediate vicinity of the diabatic crossing are characterized by large Franck–Condon factors if one uses Fermi's golden rule to treat the photodissociation process. At a certain intensity (for a given laser pulse length) all molecules in these levels will be dissociated. A further increase in intensity leads to more dissociation of levels that are not yet saturated, i.e. levels with smaller Franck–Condon factors which are predominantly states with smaller vibrational quantum numbers $v$. This in turn leads to the appearance of low kinetic energy fragments at high intensities. Therefore, the detection of these fragments is not an indication of a new effect in photodissociation. The dissociation rate for molecules that tunnel through the barrier of $E_1$ is drastically different for LIP and FGR. Fragments from molecules that took

this route of dissociation would also have low kinetic energies and a quantitative analysis of energy spectra would allow to identify these fragments and thus to establish a new phenomenon.

Lowering $kT$ to, for example, 0.03 eV reduces the contribution from levels in the region of the diabatic crossing, i.e. fewer molecules escape over the barrier of $E_1$ ( "bond-softening") and below the minimum of $E_2$. At the same time, the contribution from tunneling of low lying vibrational states (e.g. $v = 0, 1$) is increased. Thus a clear distinction between the two models in question becomes possible in a numerical simulation. If one wishes to observe stabilization, a higher temperature (and shorter laser pulses) are advantageous. Current experimental efforts in our laboratory are devoted to controlling the relative population of rovibrational levels and thus observing individually the three phenomena mentioned before.

The simulation of the experiment takes the following differential equation as a starting point:

$$\mathrm{d}N_{\lambda,v,K}(x) = -N_{\lambda,v,K}(x)\, R_{\lambda,v,K}\,(I(x,y,z),\theta)\, \mathrm{d}x\,. \qquad (1)$$

Here, $R_{\lambda,v,K}$ symbolizes the rate at which $Ar_2^+$ molecules in a given rovibrational level leave the potential system of Fig. 1 and become unbound. It depends on the laser intensity $I$ a molecule experiences. The intensity in turn is a known function of the spatial coordinates $x$, $y$, and $z$ of the center-of-mass of the molecule. Furthermore, the angle between the internuclear axis and the axis of the laser polarization ($z$-direction), $\theta$, determines the effective field strength experienced by the molecule for this parallel transition between two $\Sigma$-states. The number of molecules not dissociated by the light field is denoted by $N$. The origin of the Cartesian coordinate system lies in the center of the laser focus, and the $x$-axis points into the direction of molecular beam propagation. Integration of this differential equation with respect to $x$, $y$, $z$, and $\theta$ yields the absolute number of dissociated molecules in a given rovibrational level. The dissociation rate $R$ for each individual rovibrational level has been obtained from LIP as described in Section 2 or, alternatively, starting from FGR:

$$R_{\lambda,v,K} = \sigma_{\lambda,v,K}\frac{I}{hc/\lambda}\,, \qquad (2)$$

where $\sigma$ represents the cross section for excitation from a given rovibrational level of the ground electronic state $A\,^2\Sigma_u^+$ to the dissociative state $D\,^2\Sigma_u^+$. The following expression for $\sigma$ can be derived from FGR [31]:

$$\sigma_{\lambda,v,K} = 4.42\times 10^{-17}\frac{\varepsilon + |E_{\lambda,v,K}| + \Delta}{\sqrt{\varepsilon}}|M_{\lambda,v,K}|^2\ \mathrm{cm}^2\,. \qquad (3)$$

The total fragment energy is denoted by $\varepsilon$, and $E_{\lambda,v,K}$ stands for the binding energy of the level characterized by $v$ and rotational quantum number $K$. The fine structure splitting in the ground state of $Ar^+$ is denoted by $\delta$. The dipole matrix element $M$ between bound and continuum states is given by

$$M_{\lambda,v,K} = \int_0^\infty \chi_{v,K}(r)\chi_{\epsilon,K}(r)\mu_\Sigma(r)\,\mathrm{d}r\,, \qquad (4)$$

with $\chi_{v,K}(r)$ and $\chi_{\epsilon,K}(r)$ representing the bound and continuum nuclear wavefunctions, respectively. These wavefunctions were obtained from numerical integration of the Schrödinger equation for the movement of the nuclei under the influence of the $A\,^2\Sigma_u^+$ and $D\,^2\Sigma_g^+$ potential, respectively. The electronic dipole moment is denoted by $\mu_\Sigma(r)$ which depends on the internuclear distance $r$.

Because all relevant properties of $Ar_2^+$ have been experimentally established, $R$ is calculated precisely. As long as the relative change in intensity, $|(\mathrm{d}I/\mathrm{d}t)/I|$, is much smaller than $1/\tau$, with $\tau$ being the vibrational period, the rate $R$ obtained from LIP is well defined. This is always the case for the pulses employed in this experiment. Performing a sum over the contributions from each rovibrational level weighted according to the experimentally determined populations of these levels, and finally multiplying by the detection effiency for $Ar^+$ (also known experimentally) gives the absolute number of dissociated molecules to be compared with the experimental results in Fig. 3.

The unambiguous interpretation of the strong field data requires the determination of the relevant properties of $Ar_2^+$. Numerous theoretical and experimental studies have contributed to the knowledge of the structure of this molecule. We used the results obtained in these previous studies where applicable and relied on our own spectroscopic studies where it seemed appro-

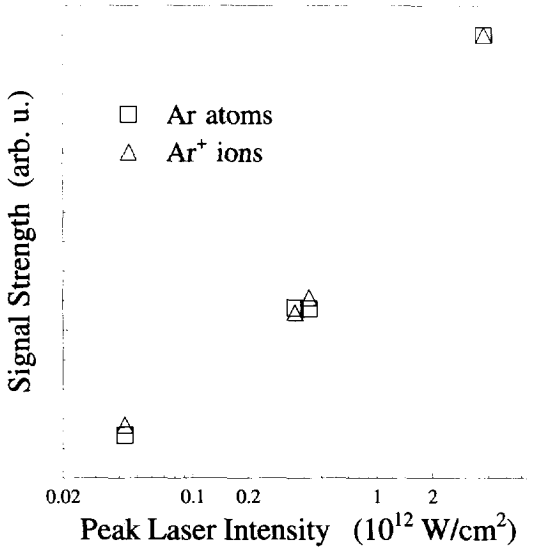


Fig. 4. Comparison of the signal strengths of simultaneously detected charged ($Ar^+$-ions) and neutral photofragments (Ar-atoms). The agreement over a wide intensity range allows to exclude multi-photon ionization of Ar or $Ar_2^+$.

priate. Thus, optimized potential curves for the $A\,^2\Sigma_u^+$ and $D\,^2\Sigma_g^+$ states, the electric dipole moment coupling these states, and also the populations of rovibrational levels in the ground state could be derived [32]. Neglecting the coupling of the ground state to other electronic states than $D\,^2\Sigma_g^+$ is well justified. This Letter is devoted to a study of strong field effects, and discussing molecular properties of $Ar_2^+$ is beyond its scope. Spectroscopic results on $Ar_2^+$ will be discussed in detail in a forthcoming publication.

In order to exclude a possible contribution to the measured $Ar^+$ signal from processes other than one-photon dissociation, we measured simultaneously the number of charged and neutral photofragments over an intensity range of two orders of magnitude (Fig. 4). If ionization of $Ar_2^+$ or of Ar atoms (photofragments) were to set in at high intensity, there would be a discrepancy between the signal strengths measured at the two detectors. This is clearly not the case (Fig. 4). A first qualitative analysis of the energy and angular distributions of the photofragments rules out multiphoton dissociation of $Ar_2^+$ and is in agreement with the interpretation of the data presented in Fig. 3. A detailed quantitative analysis of these distributions will follow in a longer publication.

## 5. Conclusion

We present an experiment on molecules in strong laser fields that, is amenable to a complete quantitative comparison to theoretical predictions. An explanation of the experimental data in terms of light-induced molecular potentials is possible, since all relevant parameters are determined experimentally and competing processes, e.g. multi-photon ionization or dissociation, are not of importance. For the particular data presented here the population of rovibrational levels favors bond-softening (due to one-photon coupling). This effect can equally well be described with Fermi's golden rule and tends to mask other phenomena caused by light-induced potentials in intense laser fields. The present results prescribe a road to the individual observation of new phenomena (cases (i)–(iii) predicted by light-induced potentials, namely control of the relative population of rovibrational levels in future experiments.

## Acknowledgement

We thank F. Rebentrost, P. Schwendner, F. Seyl, R. Schinke, J. Bestle, and W.P. Schleich for making their computational results available to us prior to publication. It is a pleasure to acknowledge fruitful discussions with P. Lambropoulos. W. Simon, K. Linner, and H. Brückner assisted in all technical matters.

## References

[1] A.D. Bandrauk, E. Aubanel and J.-M. Gauthier in: Molecules in laser fields, ed. A.D. Bandrauk (Marcel Dekker, New York, 1994) ch. 3.
[2] A. Giusti-Suzor, F.H. Mies, L.F. DiMauro, E. Charron and B. Yang, J. Phys. B 28 (1995) 309, and references therein.
[3] O. Atabek, M. Chrysos and R. Lefebvre, Phys. Rev. A 49 (1994) R8.
[4] J. Bestle and W.P. Schleich, private communication.
[5] H.P. Breuer, K. Dietz and M. Holthaus, Phys. Rev. A 45 (1992) 550.
[6] Z. Chen, M. Shapiro and P. Brumer, J. Chem. Phys. 102 (1995) 5683.
[7] T.F. George, I.H. Zimmermann, J.-M. Yuan, J.R. Laing and P.L. DeVries, Accounts Chem. Res. 10 (1977) 449.
[8] A.D. Hammerich and R. Kosloff, J. Chem. Phys. 97 (1992) 6410.
[9] T.F. Jiang, Phys. Rev. A 48 (1993) 3995.

[10] A.M.F. Lau and C.K. Rhodes, Phys. Rev. A 16 (1977) 2392.
[11] S. Manoli and T.T. Nguyen-Dang, Phys. Rev. A 48 (1993) 4307.
[12] S. Miret-Artès and D.A. Micha, Phys. Rev. A 48 (1993) R4059.
[13] A.I. Pegarkov and L.P. Rapoport, Optika i Spektroskopiya 65 (1988) 55.
[14] F. Rebentrost, private communication.
[15] P. Schwendner, F. Seyl and R. Schinke, private communication.
[16] A.I. Voronin and A.A. Samokhin, Soviet Phys. JETP 43 (1976) 4.
[17] G. Yao and S.-I. Chu, Phys. Rev. A 48 (1993) 485.
[18] P.H. Bucksbaum, A. Zavriyev, H.G. Muller and D.W. Schumacher, Phys. Rev. Letters 64 (1990) 1883.
[19] A. Zavriyev, P.H. Bucksbaum, H.G. Muller and D.W. Schumacher, Phys. Rev. A 42 (1990) 5500.
[20] S.W. Allendorf and A. Szöke, Phys. Rev. A 44 (1991) 518.
[21] K. Codling and L.J. Frasinski, J. Phys. B 26 (1993) 783, and references therein.
[22] P. Dietrich and P.B. Corkum, J. Chem. Phys. 97 (1992) 3187.
[23] F.A. Ilkov, S. Turgeon, T.D.G. Walsh, and S.L. Chin, Chem. Phys. Letters 247 (1995) 1.
[24] G.R. Kumar, C.P. Safvan, F.A. Rajgara and D. Mathur, J. Phys. B 27 (1994) 2981.
[25] M. Schmidt, D. Normand and C. Cornaggia, Phys. Rev. A 50 (1994) 5037.
[26] H.D. Bovensmann gen. Schröer and E. Tiemann, Z. Physik D 35 (1995) 19.
[27] J.W.J. Verschuur, L.D. Noordam and H.B. van Linden van den Heuvell, Phys. Rev. A 40 (1989) 4383.
[28] C. Wunderlich, V. Betz, R. Bruckmeier and H. Figger, J. Chem. Phys. 98 (1993) 9362.
[29] C. Zener, Proc. Roy. Soc. A 137 (1932) 696.
[30] C. Zhu and H. Nakamura, J. Chem. Phys. 101 (1994) 10630.
[31] G.H. Dunn, Phys. Rev. 172 (1968) 1.
[32] C. Wunderlich, Ph.D. Thesis, Ludwig-Maximilians-Universität München (1995), unpublished.